HELDA
HELSINGIN YLIOPISTO
HELSINGFORS UNIVERSITET
UNIVERSITY OF HELSINKI

UNIVERSITY OF HELSINKI

https://helda.helsinki.fi

Total alkalinity production in a mangrove ecosystem reveals an overlooked Blue Carbon component

Saderne, Vincent

2021-04

Saderne , V , Fusi , M , Thomson , T , Dunne , A , Mahmud , F , Roth , F , Carvalho , S & Duarte , C M 2021 , ' Total alkalinity production in a mangrove ecosystem reveals an overlooked Blue Carbon component ' , Limnology and oceanography letters , vol. 6 , no. 2 , pp. 61-67 . https://doi.org/10.1002/lol2.10170

http://hdl.handle.net/10138/333427
https://doi.org/10.1002/lol2.10170

cc_by
publishedVersion

Downloaded from Helda, University of Helsinki institutional repository.

This is an electronic reprint of the original article.

This reprint may differ from the original in pagination and typographic detail.

Please cite the original version.

Check for updates

LIMNOLOGY AND OCEANOGRAPHY
Letters

ASLO
Open Access

Limnology and Oceanography Letters 2020
© 2020 The Authors. *Limnology and Oceanography Letters* published by Wiley Periodicals LLC on behalf of Association for the Sciences of Limnology and Oceanography.
doi: 10.1002/lol2.10170

LETTER

Total alkalinity production in a mangrove ecosystem reveals an overlooked Blue Carbon component

Vincent Saderne[1]*, *Marco Fusi*[2], *Timothy Thomson*[3], *Aislinn Dunne*[1], *Fatima Mahmud*[4], *Florian Roth*[5,6], *Susana Carvalho*[1], *Carlos M. Duarte*[1,7]

[1]King Abdullah University of Science and Technology, Red Sea Research Center, Thuwal, 23955-6900, Saudi Arabia; [2]Edinburgh Napier University, School of Applied Sciences, Edinburgh, UK; [3]School of Science, University of Waikato, Tauranga, New Zealand; [4]University of California, Berkeley, USA; [5]Stockholm University, Baltic Sea Centre, Stockholm, Sweden; [6]University of Helsinki, Tvärminne Zoological Station, Helsinki, Finland; [7]King Abdullah University of Science and Technology, Computational Bioscience Research Center, Thuwal, 23955-6900, Saudi Arabia

Scientific Significance Statement

Blue Carbon ecosystems (seagrass meadows, mangroves, and saltmarshes) sequester atmospheric CO_2 as organic carbon in their sediments for periods of centuries to millennia. Calcium carbonate ($CaCO_3$) dissolution is another major permanent sinks of atmospheric CO_2 in the coastal area, but has been disregarded in Blue Carbon ecosystems. In the Red Sea, as in many tropical areas, Blue Carbon ecosystems thrive on carbonate sediment generated by the erosion of coral reefs. Our study reveals that the dissolution of $CaCO_3$ is a major sink of atmospheric CO_2 in carbonate sediment mangroves, representing 23-fold the sink from organic carbon sequestration at our Red Sea mangrove site. The $CaCO_3$ calcification and dissolution budget should be considered in future Blue Carbon assessments.

Abstract

Mangroves have the capacity to sequester organic carbon (C_{org}) in their sediments permanently. However, the carbon budget of mangroves is also affected by the total alkalinity (TA) budget. Principally, TA emitted from carbonate sediment dissolution is a perennial sink of atmospheric CO_2. The assessment of the TA budget of mangrove carbonate sediments in the Red Sea revealed a large TA emission of 403 ± 17 mmol m^{-2} d^{-1}, independent of light, seasons, or the presence of pneumatophores, compared to -36 ± 10 mmol m^{-2} d^{-1} in lagoon sediment. We estimate the TA emission from carbonate dissolution in Red Sea mangroves supported a CO_2 uptake of 345 ± 15 gC m^{-2} yr^{-1}, 23-fold the C_{org} burial rate of 15 gC m^{-2} yr^{-1}. The focus on C_{org} burial in sediments may substantially underestimate the role of mangroves in CO_2 removal. Quantifying the role of mangroves in climate change mitigation requires carbonate dissolution to be included in assessments.

*Correspondence: vincent.saderne@kaust.edu.sa

Associate editor: Catherine Ellen Lovelock

Author Contribution Statement: VS and MF designed the study. VS, MF, TT, AD, FR, and FM carried out field and laboratory work. VS and MF analyzed the data. VS wrote the first draft. All authors contributed to drafting and improving the manuscript and approved the submission.

Data Availability Statement: The data are archived in the online repository Pangaea.de. https://doi.org/10.1594/PANGAEA.922761.

Additional Supporting Information may be found in the online version of this article.

This is an open access article under the terms of the Creative Commons Attribution License, which permits use, distribution and reproduction in any medium, provided the original work is properly cited.

Mangrove ecosystems, along with seagrass beds and saltmarshes, sequester large amounts of organic carbon (C_{org}) in their sediments (Duarte et al. 2005, 2013; Mcleod et al. 2011). Carbon burial in mangrove sediments has been estimated at 21 to 32.4 Tg C_{org} yr^{-1} globally (Breithaupt et al. 2012), contributing about 10% of the C_{org} burial in the ocean (Duarte et al. 2005; Breithaupt et al. 2012). Before perennial sequestration, part of the labile fraction of the organic matter (OM) is remineralized through a cascade of redox reactions involving aerobic respiration in surface sediments and hydrolysis and fermentation in the deeper layers (Middelburg 2018).

Degradation of OM in marine sediment can also be a source of total alkalinity (TA) to the marine environment. TA, simplified as the charge balance of conservative ions in seawater (e.g., Na^+, Ca^{2+}, K^+, Cl^-) and of the redox state of some minor elements (e.g., species of the nitrogen and phosphorus cycle) (Middelburg et al. 2019), is a key parameter affecting the seawater inorganic carbon system and the global carbon cycle (Krumins et al. 2013). Seawater is slightly depleted of conservative anions compared to conservative cations, and the difference (about 2 mmol kg^{-1} over a total amount of ions of the order of 600 mmol kg^{-1}), allows for the uptake of atmospheric CO_2, stored in seawater as HCO_3^- and CO_3^{2-}. The consequence of this minor imbalance results in the world's oceans storing about 98% of the CO_2 present in the atmosphere – hydrosphere system.

TA in mangrove sediments is produced through sulfate reduction, calcium carbonate ($CaCO_3$) dissolution, denitrification, and ammonification (Krumins et al. 2013). In carbonate, iron-depleted sediments characteristics of coral reefs regions (Ku et al., 1999; Hu and Burdige, 2007; Krumins et al., 2013), the TA produced from sulfate reduction is re-uptaken in equal amounts during sulfite oxidation after diffusion into the water column. Hence, much of sediment TA emissions derive from $CaCO_3$ dissolution along with denitrification and ammonification (Krumins et al. 2013). The emission of TA to the water column by mangrove sediments is a sink of atmospheric CO_2 (Maher et al. 2018). In particular, TA emission from $CaCO_3$ dissolution is a perennial sink of CO_2 at the geological time scale (Ridgwell and Zeebe 2005), which should be added to the classical assessment of Blue Carbon as C_{org} sequestration. Understanding the role of calcification and $CaCO_3$ dissolution in affecting CO_2 budgets of Blue Carbon ecosystems is a major challenge for Blue Carbon science (Macreadie et al. 2017; Saderne et al. 2019b). Through TA emission, the dissolution of $CaCO_3$ results in an atmospheric uptake of ~ 0.6 mol of CO_2 per mole of $CaCO_3$ dissolved under current atmospheric CO_2 partial pressure (pCO_2). This is independent of the pathway involved in the dissolution or metabolic activities occurring in parallel in the ecosystem (e.g., respiration, photosynthesis) (Frankignoulle et al. 1995). The CO_2 produced by the degradation of sediment OM, together with organic acid exuded by mangrove roots (Jiang et al. 2017), results in an acidification of the pore waters and the dissolution of $CaCO_3$ (Hu and Burdige 2007). Dissolution of $CaCO_3$ could also occur at the sediment-water column interface in Blue Carbon ecosystems, due to the acidification caused by the metabolic activity of the benthic fauna and flora, principally respiration at night (Rosentreter et al. 2018; Saderne et al. 2019a). Hence, based on a review of carbonate burial and budgets in Blue Carbon sediments, we recently proposed that carbonate dissolution may be an important, but overlooked mechanism of CO_2 removal in Blue Carbon habitats where carbonate is supplied from adjacent calcifying ecosystems, such as coral reefs and lithogenic carbonate deposits (Saderne et al. 2019b). Here, we report a high rate of CO_2 removal from TA net emission by a mangrove stand with carbonate-rich sediments (80% $CaCO_3$ of dry weight; Saderne et al. 2018) in the central-eastern Red Sea. We do so based on assessments of annual net TA fluxes in a flooded mangrove stand compared to those in bare reef lagoon sediments outside of the mangrove.

Materials and methods

Site

The incubations were conducted in a mono-specific *Avicennia marina* mangrove swamp of the central Red Sea (22°20′23″N, 39°05′22″E, Fig. 1), in the King Abdullah University of Science and Technology Ibn Sina field research station and conservation area (Saudi Arabia). Coastal expansion of mangrove in the Red Sea is limited by the small tidal range, approximately 20–30 cm in the central part of the Red Sea, combined with seasonal variations of water level, decreasing from May to August of approximately 50 cm and re-increasing thereafter till October, exposing mangroves to increasing period of emersion throughout summer (Pugh and Abualnaja 2015). The water column in our site classically varies between complete emersion and $\sim$ 30–40 cm depending on the tide and period of the year, which is representative of Red Sea mangroves. Red Sea mangroves thrive in one of the driest areas of the planet, with precipitations ranging from 10 to

Fig. 1. Location of the incubation (lagoon and mangrove) sites in the Red Sea.

25 mm per month on average in 2018 (Global Precipitation Climatology Centre).

Mangrove incubations

The incubations were conducted during the last 2 h of the rising tide, around solar noon and at night within the same day, to distinguish between light and dark fluxes of TA and dissolved inorganic carbon (DIC). The incubations were conducted from April 2018 to May 2019. In April/May 2018, day and night incubations were done 15 d apart.

The incubation chambers in the mangrove consisted of transparent PVC pipes, open on both ends, enclosing a sediment surface of 71 cm^2 (9.5 cm diameter). The mean (± SD) volume of water in the chambers at the start of the incubations was 1.2 ± 0.4 L (height of 16.7 ± 5.4 cm) and increased by 0.20 ± 0.18 L (2.8 ± 2.6 cm) during the incubation, due to the rising tide.

This incubation method, with chambers open on both sides, allows the natural pore-water advective flow of compounds from the sediment to the water column. The problem of reproducing natural advection in benthic incubation systems is a key issue in the estimate of sediment – water fluxes (Tengberg et al., 2004). This is traditionally achieved through the generation of a rotary current within the chamber, creating a central depression pulling the solutes out of the sediment (Tengberg et al., 2004). The fluxes measured are then partly depending on the stirring force imposed in the chamber (Tengberg et al., 2004). In our mangrove incubations, the advection of the solutes from the sediment is ensured by the natural rise of water in the chambers during the rising tide.

The mean (± SD) duration of the incubations was 1.48 ± 0.22 h. Incubations of bare mangrove sediment and of bare sediment (without animal burrows) with one pneumatophore, tall enough to emerge from the water, were conducted. Each incubation event (for each day, night, and at different seasons) included 10 mangrove and 10 pneumatophore sediment incubations. Samples (100 mL) were taken at the beginning and end of incubations in each chamber for TA and DIC measurements. In parallel, samples were taken at the beginning and end of the incubation period in surface water outside of the mangrove as reference. Samples were poisoned after collection with $HgCl_2$ (Dickson et al. 2007).

Two conductivity – temperature – depth (CTD) sensors (Exo1, YSI Inc., Yellow Springs, USA) were installed in the mangrove at the incubation site and outside at the reference sampling point.

Bare lagoon sediment incubations

To test whether TA fluxes in mangrove sediments differ from adjacent unvegetated reef lagoon sediments, we carried out incubations with closed benthic chambers in parallel to the mangrove incubations on the 16.01.2019 and 25.05.2019, at daytime and nighttime, in 1–1.5 m water depth. The closed benthic incubation chambers were cylindrical, made of transparent polymethyl methacrylate, with a diameter of 0.5 m, a height of 0.39 m, a volume of 0.68 m^3, and covered a sediment surface of 0.2 m^2. A pump in each chamber was placed to ensure the mixing of water and advection from sediment. A detailed description of the chambers and pumping systems can be found in Roth et al. (2019a). Samples for CO_2 system determinations were taken at the beginning and end of incubations (incubation time of 104–124 min). Samples were transferred to glass bottles and poisoned with $HgCl_2$ right after collection (Dickson et al. 2007).

Sample analysis

TA was measured using a dedicated open-cell titration instrument (AS-ALK2, Apollo SciTech). DIC was measured with an AS-C3 analyzer (Apollo SciTech) by infrared absorption spectrometry in the air phase after complete conversion into $CO_{2(g)}$ by acidification of the sample. The instruments were calibrated on every measurement day using certified CO_2 in seawater reference material (A. Dickson, Scripps Institution of Oceanography, La Jolla, California). Based on a global inter-calibration effort conducted in 2017 by A. Dickson and E. Bockmon (Scripps Institution of Oceanography, La Jolla, California), we estimate the mean ± SD accuracy of our measurements to be 0.21 ± 1.93 μmol TA kg^{-1} and −3.34 ± 2.2 μmol DIC kg^{-1}. The salinity was measured in each sample using an Exo conductivity sensor (YSI).

Calculations

For each mangrove incubation, the TA production rate, in mmol m^{-2} h^{-1} was determined as the change of the total amount of TA (ΔTA_{tot}, in mmol) in the enclosed water column, from which the variation of TA due to changes in salinity (ΔTA_{sal} in mmol) was subtracted. The variation in salinity could be due to dilution/concentration with water from incoming tide, from advection of hypersaline pore water or due to evaporation. The relationship between TA and salinity is considered linear in seawater, and therefore any change in salinity causes a proportional change in TA.

$$\Delta TA_{tot} = TA_f \, V_f \, \rho_f - TA_i \, V_i \, \rho_i \quad (1)$$

With TA_i and TA_f are the TA in mmol kg^{-1} at the beginning and end of incubation, respectively; V_i and V_f are the initial and final volumes of water in the chamber at the beginning and end of incubation (in liter), calculated from the water column height in the chamber using basic cylinder volume formula; ρ is the volumic mass (kg L^{-1}) of seawater derived from the samples salinity and CTD temperature.

TA_{sal} is estimated using a TA to salinity ratio R (mmo kg^{-1} psu^{-1}) of incoming tidal water, from measurements in the reference sample, taken in surface water outside the mangrove.

$$R = \frac{TA_{ref}}{S_{ref}} \quad (2)$$

$$\Delta TA_{sal} = R\,V_f\,S_f\,\rho_f - R\,V_i\,S_i\,\rho_i \quad (3)$$

With S_{ref}, S_i, and S_f are the salinities in the reference, initial, and final samples.

$$TA_{prod} = \frac{\Delta TA_{tot} - \Delta TA_{sal}}{\Delta t.\text{Area}} \quad (4)$$

With Δt is the duration of the incubation as the difference between the initial and final time (t_i and t_f) in hours.

The method for the calculation of DIC production rates is presented in Supplementary Material and Method. See the DIC production rates in Supplementary Fig. S1.

Statistical analysis

To test the differences of our response variable TA, a fully factorial permutational multivariate ANOVA was used, considering our explanatory variable the daytime (two levels: day and night), the Season (three levels: Spring 2018, Winter 2018/2019 and Spring 2019), the type of sediment (two levels, pneumatophores, and bulk) (Supplementary Tables S1–S3). Prior to the analysis, normality of the data was tested. Euclidean distance was used to generate the dissimilarity matrix for the response variable TA. The analysis was performed using the function *adonis2*() in the "R" package "vegan" (Oksanen et al. 2019), and for pairwise comparison, the "R" package pairwiseAdonis (Martinez Arbizu 2019).

Result and discussion

TA production rates in Red Sea mangroves

The mean (± SE) net TA emission rates during daytime in the bare mangrove sediment and mangrove pneumatophore stands were 16.3 ± 2.7 and 15.4 ± 1.9 mmol m^{-2} h^{-1}, respectively, similar to the net TA emission rates at nighttime (17.3 ± 1.6 and 18.3 ± 2 mmol m^{-2} h^{-1} in bare sediment and mangrove pneumatophores, Fig. 2a). Neither the time of day nor the presence of a pneumatophore significantly influenced the TA fluxes (all $p > 0.05$; Table S1). In contrast, bare sediments in the adjacent lagoon were net sinks of TA at daytime with a mean (± SE) emission rates of -2.5 ± 0.9 mmol m^{-2} h^{-1} (Fig. 2a; Table S2). There was no clear pattern of emission or uptake of TA in the lagoon at nighttime (0.32 ± 0.6 mmol m^{-2} h^{-1}; Fig. 2a; Table S2). Although we did not find an apparent seasonal pattern in our data (Fig. 2b), we found significant changes over time ($p = 0.001$; Table S1), which differed between sediment types (bare mangrove sediment, sediment with pneumatophore and bare lagoon sand) and the time of the day (both $p < 0.01$; Table S1). Pooling together the two mangrove treatments (pneumatophore and bare sediment), all incubation events, and considering 12-h light : 12-h dark daily cycles, the mean (± SE) daily flux of TA from our mangrove site was 403 ± 17 mmol m^{-2} d^{-1}. This would correspond to an estimated yearly production of 147 ± 6 or 115 ± 5 mol TA m^{-2} yr^{-1} considering that the sediments in the mangrove stand are emerged 22% of the year (based on 2016–2017 time series from Saderne et al., 2019a).

The TA emission rates in the Red Sea mangrove reported here are higher than any rates previously reported, all in Australian mangroves (Faber et al. 2014; Sippo et al. 2016; Maher et al. 2018; Santos et al. 2019). Those studies estimated TA fluxes from sediment pore water sampling (^{222}Rn mass balance technique; Faber et al. 2014; Santos et al. 2019) and/or at the scale of entire mangrove creeks or inlets using hydrological models coupled with 24 h seawater sampling (Faber et al. 2014; Sippo et al. 2016; Maher et al. 2018; Santos et al. 2019). From pore water, Faber et al. (2014) reported TA fluxes of 310 and 46 mmol m^{-2} d^{-1} in two mangroves inlets of Victoria (Australia) and estimated that the contribution of carbonate dissolution to this flux to be rather negligible (about 0.8%). Santos et al. (2019) measured a mean pore water

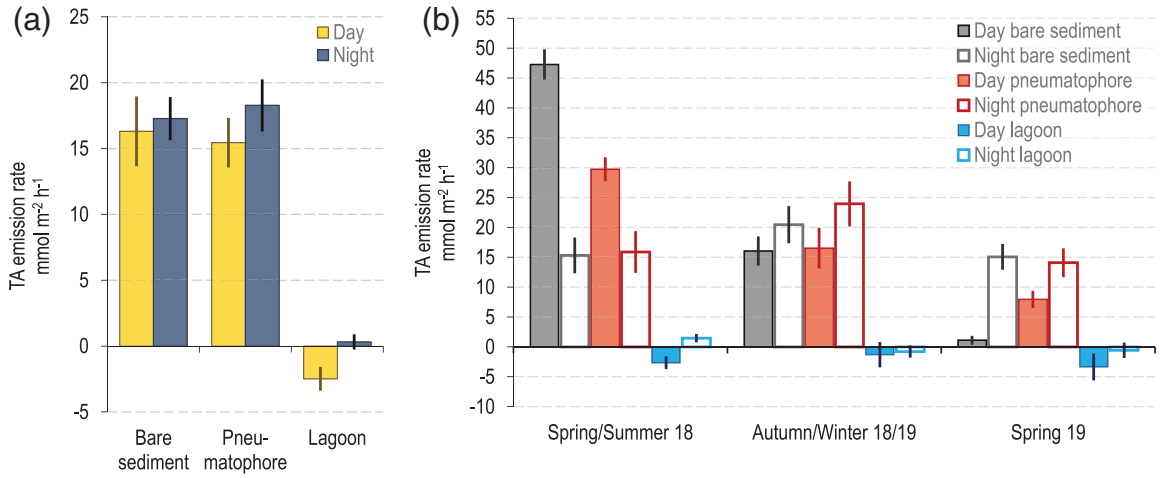

Fig. 2. Net TA emissions rates. Mean ± SE hourly emission rates of TA (mmol m^{-2} h^{-1}); (**a**) at daytime and nighttime in mangrove bare sediment and pneumatophore incubations, and in lagoon sand incubations summarized by type of sediments; (**b**) summarized by seasons at day and night.

TA flux of 124 ± 131 mmol m^{-2} d^{-1} from four sampling events in 2012–2013 in a mangrove of New South Wales (Australia). In parallel, they used hydrological models to estimate the TA export rates of the two mangrove inlets to be on average 12 ± 6 mmol m^{-2} d^{-1}. From hydrological modeling, another study in south Queensland (Australia) reported TA export rates of 96 ± 35 mmol m^{-2} d^{-1} from a mangrove inlet (Maher et al. 2018). Sippo et al. (2016) reported TA export rates to the coastal zone from six mangrove creeks along a latitudinal gradient from 38°S to 12°S along the eastern Australian coast (southern Victoria to Darwin) ranging from −1 to 116 mmol m^{-2} d^{-1}. From these values and considering the global coverage of mangroves, they estimated a global TA export from mangrove ecosystems to the coastal ocean of 67 mmol m^{-2} d^{-1}, six-fold lower than the TA production rate we measured for the central Red Sea mangrove stand studied here (i.e., 403 ± 17 mmol m^{-2} d^{-1}).

CO_2 removal by carbonate dissolution as a key process in mangroves on carbonate platforms

The mangroves of the Red Sea have one of the lowest C_{org} burial rates reported in the world (15 g C_{org} m^{-2} yr^{-1}; Almahasheer et al. 2017), 10 times lower compared to the mean global estimate of 163 g C_{org} m^{-2} yr^{-1} (Breithaupt et al. 2012). However, this estimate does not account for the atmospheric CO_2 supported by TA emissions of mangrove sediments.

The carbonate–silicate geochemical cycle is a major driver of the earth's climate at the geological time scale (Ridgwell and Zeebe 2005). It regulates the atmospheric pCO_2, and, therefore, controls the earth's temperature through modulation of the greenhouse effect (the carbonate–silicate thermostat). A key aspect of this cycle is the segregation and emission of TA by biogenic calcification and carbonate dissolution, regulating the capacity of the oceans to retain atmospheric CO_2 as DIC. Thus, CO_2 uptake supported by TA emissions from the dissolution of carbonate reservoirs contributes to mitigating climate change (Saderne et al. 2019b). Mangroves that are candidates to increase their climate change mitigation capacity from TA emissions include, therefore, those growing on carbonate platforms (Saderne et al. 2019b).

Carbonate platforms created by the accumulation of the shells and skeletons of marine calcifiers over tens of thousands to millions of years represent fossilized TA reservoirs. When carbonate sands supplied by geological carbonate reservoirs dissolve due to the acidification of the sediments in mangrove ecosystems, this fossilized TA is reemitted to the water column. Subsequent equilibration with the atmosphere leads to an uptake of 0.6–0.7 mol of CO_2 per dissolved mole of $CaCO_3$ (Frankignoulle et al. 1995; Abril and Frankignoulle 2001). The next highest source of TA emission from the sediment is linked to the transformations of nitrogen in relation to OM degradation, net ammonification (ammonification minus nitrification), and denitrification (Krumins et al. 2013). These emissions can be associated with the C_{org} cycle. Including them into Blue Carbon assessments would require an estimate of the net TA generated during the cycle of primary production vs. OM degradation. The relationship between TA and DIC emission rates (Fig.3) confirms that the emitted TA does not solely originate from the dissolution of $CaCO_3$ but from a combination of dissolution and redox processes (Fig. 3). However, we cannot determine the proportion of TA resulting from $CaCO_3$ dissolution. The partitioning between the sources of TA emitted from Blue Carbon sediment remains a scientific and analytical challenge to date and requires further investigations.

Hence, considering that 65% of the TA production in reef, bank, and bay sediments is supported by carbonate dissolution (Krumins et al. 2013) and that one mole of $CaCO_3$ dissolved results in the uptake of 0.6 mol of CO_2, the mean TA mangrove production rate found in our study (147 ± 6 mol m^{-2} yr^{-1}) would be equivalent to an atmospheric uptake of 345 ± 15 g C m^{-2} yr^{-1}. This sink is 23-fold larger than the C_{org} burial rate for central Red Sea mangroves estimated at 15 g C m^{-2} yr^{-1} (Almahasheer et al. 2017). In comparison, in a carbonate poor mangrove of Australia (less than 1% sediment DW), the carbon sink from TA export was estimated 1.7-fold larger than OC burial rates (Sanders et al. 2016; Maher et al. 2018). The central Red Sea mangrove studied here would reach a carbon sink value of 360 g C m^{-2} yr^{-1}, which is 2.2-fold above global mangrove mean based on C_{org} alone, estimated at 163 g C m^{-2} yr^{-1} (Breithaupt et al. 2012). The assumption that only 65% of the

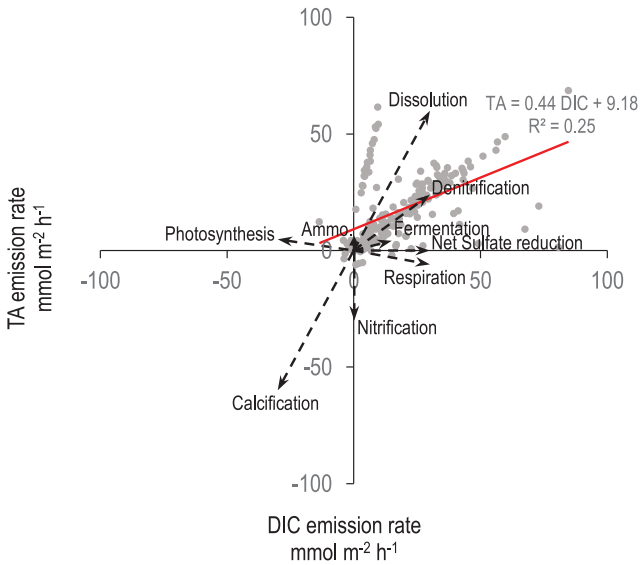

Fig. 3. Stochiometry between DIC and TA emission rates in mangrove incubations. Data are the TA to DIC sediment emission rates for all incubations performed (day, night, all seasons). Red line: Linear regression between TA and DIC ($F = 66$, $p < 0.0001$, slope and intercept $p < 0.0001$). Vectors of relative length represent the TA to DIC stoichiometry of the main chemical processes occurring in sediments. Ammo.: ammonification.

TA mangrove production comes from carbonate dissolution, compared to 100% assumed in many studies (e.g., Van Dam et al. 2019 in seagrass meadows), renders our estimate of 345 ± 15 g C m^{-2} yr^{-1} of CO_2 removed from TA emission in the Red Sea mangroves a conservative one.

The dissolution rates found in our mangrove site can be compared to calcification rates observed in nearby coral reefs, a process that emits large amounts of CO_2 to the atmosphere globally (Frankignoulle et al. 1995; Borges et al. 2005). Roth et al. (2019b) found mean (± SE) net calcification rates of 4.8 ± 0.4 kg $CaCO_3$ m^{-2} yr^{-1} in an adjacent coral reef, equivalent to a CO_2 emission of 344 ± 26 g C m^{-2} yr^{-1}. The CO_2 uptake by carbonate dissolution in 1 ha of Red Sea mangrove, therefore, compensates for the CO_2 production by calcification of 1 ha of Red Sea coral reef. Mangrove ecosystems are often growing on underlying carbonate platforms, principally due to the presence of extant and fossil coral reefs in the same latitudes (Saderne et al. 2019b). Our results indicate that assessments of the Blue Carbon potential of mangroves need be extended to consider CO_2 removal from the TA emission in mangrove stands on carbonate deposits. Likewise, targeting mangroves along carbonate deposits for restoration and expansion increases the potential climate change mitigation of mangrove restoration projects.

Conflict of interests

The authors declared no potential conflict of interests.

References

Abril, G., and M. Frankignoulle. 2001. Nitrogen-alkalinity interactions in the highly polluted scheldt basin (Belgium). Water Res. **35**: 844–850. doi:10.1016/S0043-1354(00)00310-9.

Almahasheer, H., O. Serrano, C. M. Duarte, A. Arias-Ortiz, P. Masque, and X. Irigoien. 2017. Low carbon sink capacity of Red Sea mangroves. Sci. Rep. **7**: 1–10. doi:10.1038/s41598-017-10424-9.

Borges, A. V., B. Delille, and M. Frankignoulle. 2005. Budgeting sinks and sources of CO_2 in the coastal ocean: Diversity of ecosystem counts. Geophys. Res. Lett. **32**: 1–4. doi:10.1029/2005GL023053.

Breithaupt, J. L., J. M. Smoak, T. J. Smith, C. J. Sanders, and A. Hoare. 2012. Organic carbon burial rates in mangrove sediments: Strengthening the global budget. Global Biogeochem. Cycles **26**: 2012GB004375. doi:10.1029/2012GB004375.

Van Dam, B. R., C. Lopes, C. L. Osburn, and J. W. Fourqurean. 2019. Net heterotrophy and carbonate dissolution in two subtropical seagrass meadows. Biogeosciences **16**: 4411–4428. doi:10.5194/bg-16-4411-2019.

Dickson, A. G., C. L. Sabine, and J. R. Christian. 2007, *Guide to best practices for ocean CO_2 measurements*. North Pacific Marine Science Organization.

Duarte, C. M., I. J. Losada, I. E. Hendriks, I. Mazarrasa, and N. Marbà. 2013. The role of coastal plant communities for climate change mitigation and adaptation. Nat. Clim. Chang. **3**: 961–968. doi:10.1038/nclimate1970.

Duarte, C. M., J. J. Middelburg, and N. Caraco. 2005. Major role of marine vegetation on the oceanic carbon cycle. Biogeosciences **2**: 1–8. doi:10.5194/bg-2-1-2005.

Faber, P. A., V. Evrard, R. J. Woodland, I. C. Cartwright, and P. L. M. Cook. 2014. Pore-water exchange driven by tidal pumping causes alkalinity export in two intertidal inlets. Limnol. Oceanogr. **59**: 1749–1763. doi:10.4319/lo.2014.59.5.1749.

Frankignoulle, M., M. Pichon, and J.-P. Gattuso. 1995. Aquatic calcification as a source of carbon dioxide, p. 265–271. *In*, *Carbon sequestration in the biosphere*. Berlin, Heidelberg: Springer.

Hu, X., and D. J. Burdige. 2007. Enriched stable carbon isotopes in the pore waters of carbonate sediments dominated by seagrasses: Evidence for coupled carbonate dissolution and reprecipitation. Geochim. Cosmochim. Acta **71**: 129–144. doi:10.1016/j.gca.2006.08.043.

Jiang, S., F. Xie, H. Lu, J. Liu, and C. Yan. 2017. Response of low-molecular-weight organic acids in mangrove root exudates to exposure of polycyclic aromatic hydrocarbons. Environ. Sci. Pollut. Res. **24**: 12484–12493. doi:10.1007/s11356-017-8845-4.

Krumins, V., M. Gehlen, S. Arndt, P. Van Cappellen, and P. Regnier. 2013. Dissolved inorganic carbon and alkalinity fluxes from coastal marine sediments: Model estimates for different shelf environments and sensitivity to global change. Biogeosciences **10**: 371–398. doi:10.5194/bg-10-371-2013.

Ku, T. C. W., L. M. Walter, M. L. Coleman, R. E. Blake, and A. M. Martini. 1999. Coupling between sulfur recycling and syndepositional carbonate dissolution: Evidence from oxygen and sulfur isotope composition of pore water sulfate, South Florida Platform, U.S.A. Geochim. Cosmochim. Acta **63**: 2529–2546. doi:10.1016/S0016-7037(99)00115-5.

Macreadie, P. I., O. Serrano, D. T. Maher, C. M. Duarte, and J. Beardall. 2017. Addressing calcium carbonate cycling in blue carbon accounting. Limnol. Oceanogr. Lett. **2**: 195–201. doi:10.1002/lol2.10052.

Maher, D. T., M. Call, I. R. Santos, and C. J. Sanders. 2018. Beyond burial: Lateral exchange is a significant atmospheric carbon sink in mangrove forests. Biol. Lett. **14**: 20180200. doi:10.1098/rsbl.2018.0200.

Martinez Arbizu, P. 2019. pairwiseAdonis: Pairwise multilevel comparison using adonis. R Packag. version 0.3.

Mcleod, E., and others. 2011. A blueprint for blue carbon: Toward an improved understanding of the role of vegetated coastal habitats in sequestering CO_2. Front. Ecol. Environ. **9**: 552–560. doi:10.1890/110004.

Middelburg, J. J. 2018. Reviews and syntheses: To the bottom of carbon processing at the seafloor. Biogeosciences **15**: 413–427. doi:10.5194/bg-15-413-2018.

Middelburg, J. J., K. Soetaert, and M. Hagens. 2019. Ocean alkalinity, buffering and biogeochemical processes. Rev. Geophys. **58**: 1–43. doi:10.1002/essoar.10501337.1.

Oksanen, J., and others. 2019. Package "vegan" title community ecology package. Community Ecology. Packag. 2.5–6.

Pugh, D. T., and Y. Abualnaja. 2015. Sea-Level Changes, p. 317–328. *In The Red Sea*, Berlin, Heidelberg: Springer.

Ridgwell, A., and R. E. Zeebe. 2005. The role of the global carbonate cycle in the regulation and evolution of the earth system. Earth Planet. Sci. Lett. **234**: 299–315. doi:10.1016/j.epsl.2005.03.006.

Rosentreter, J. A., D. T. Maher, D. V. Erler, R. Murray, and B. D. Eyre. 2018. Seasonal and temporal CO_2 dynamics in three tropical mangrove creeks – A revision of global mangrove CO_2 emissions. Geochim. Cosmochim. Acta **222**: 729–745. doi:10.1016/j.gca.2017.11.026.

Roth F., C. Wild, and S. Carvalho. 2019*a*. An in situ approach for measuring biogeochemical fluxes in structurally complex benthic communities. Methods Ecol. Evol. **10**: 712–725. doi:10.1111/2041-210X.13151.

Roth, F., N. Rädecker, S. Carvalho, C. M. Duarte, and V. Saderne. 2019*b*. High summer temperatures amplify functional differences between coral- and algal-dominated reef communities. Ecology. In press.

Saderne, V., K. Baldry, A. Anton, S. Agustí, and C. M. Duarte. 2019*a*. Characterization of the CO_2 system in a coral reef, a seagrass meadow, and a mangrove forest in the central Red Sea. J. Geophys. Res. Ocean. **2**: 7513–7528. doi:10.1029/2019JC015266.

Saderne, V., and others. 2018. Accumulation of carbonates contributes to coastal vegetated ecosystems keeping pace with sea level rise in an arid region (Arabian peninsula). J. Geophys. Res. Biogeosci. **123**: 1498–1510. doi:10.1029/2017JG004288.

Saderne, V., and others. 2019*b*. Role of carbonate burial in blue carbon budgets. Nat. Commun. **10**: 1106. doi:10.1038/s41467-019-08842-6

Sanders, C. J., and others. 2016. Examining $^{239+240}$Pu, ^{210}Pb and historical events to determine carbon, nitrogen and phosphorus burial in mangrove sediments of Moreton Bay, Australia. J. Environ. Radioact. **151**: 623–629. doi:10.1016/j.jenvrad.2015.04.018.

Santos, I. R., D. T. Maher, R. Larkin, J. R. Webb, and C. J. Sanders. 2019. Carbon outwelling and outgassing vs. burial in an estuarine tidal creek surrounded by mangrove and saltmarsh wetlands. Limnol. Oceanogr. **64**: 996–1013. doi:10.1002/lno.11090.

Sippo, J. Z., D. T. Maher, D. R. Tait, C. Holloway, and I. R. Santos. 2016. Are mangroves drivers or buffers of coastal acidification? Insights from alkalinity and dissolved inorganic carbon export estimates across a latitudinal transect. Global Biogeochem. Cycles **30**: 753–766. doi:10.1002/2015GB005324.

Tengberg, A., H. Stahl, G. Gust, V. Müller, U. Arning, H. Andersson and P. O. J. Hall. 2004. Intercalibration of benthic flux chambers I. Accuracy of flux measurements and influence of chamber hydrodynamics.. Prog. Oceanogr. **60**: 1–28. doi:10.1016/j.pocean.2003.12.001.

Acknowledgments

We thank M. Predragovic, W. Rich IV, U. Langner, J. L. Curdia, R. Cadiz, and M. Ennasri for their help in the field and the lab. This research was supported by King Abdullah University of Science and Technology (KAUST) baseline funding to C.M.D. and the KAUST Circular Carbon Economy initiative.

Submitted 29 June 2020
Revised 16 September 2020
Accepted 21 September 2020